


Cite this: *RSC Adv.*, 2025, 15, 44254

Regioselective Cu(I)-catalyzed intramolecular hydroacylation and dimerization of propargylarylaldehydes

Zahra Tanbakouchian,^a Mohammad Ali Zolfigol,^a Maryam-Sadat Tonekaboni,^b Anna Kozakiewicz-Piekarz^c and Rahman Bikas^d

We present the details of the formation of regioselective C–C bonds from propargyl arylaldehydes. The readily available CuSO₄·5H₂O salt could promote regioselective intramolecular hydroacylation and head-to-head additive dimerization of propargyl aryl aldehydes in the presence of a catalytic amount of ascorbic acid. The transformations do not require any bases during the course of the reaction. In both transformations, substrates bearing electron-donating groups on the aryl ring are more compatible with the reaction conditions, providing the corresponding coupling products with good yields. In addition, the presented catalytic system shows high regioselectivity control for different substituents regardless of their polarity.

Received 3rd October 2025
Accepted 5th November 2025

DOI: 10.1039/d5ra07533e

rsc.li/rsc-advances

Introduction

Highly atom-economy methods for the formation of C–C bonds have received special attention and importance in synthetic organic chemistry. Metal-catalyzed hydroacylation is an efficient atom-economy process, which leads to the generation of α,β -unsaturated enones through alkyne–aldehyde coupling. Indeed, the overall process involves the combination of chemoselective C(sp²)–H activation coupled and C–C bond formation to afford the ubiquitous structural motif in organic synthesis. The regio- and stereoselective hydroacylation of alkynes with aldehydes can produce three isomers of α,β -enones that involve branched as well as linear *E*- and *Z*, α,β -enones. One of the limitations of this method is reductive decarbonylation, which can be prevented by using chelating moiety-bearing substrates.^{1–4} The chelation-controlled processes have become a prevailing tool to achieve regio- and enantioselective reactions under mild conditions.⁵ In 2018, Weller *et al.* reported the intermolecular hydroacylation of 2,2-dimethyl-3-morpholino-3-oxopropanal with 1-octyne catalyzed by [Rh(*cis*- κ^2 -P,P-DPEPhos) (acetone)₂][BAR₄F] at 25 °C, which provides the enones **1a/1b** (15 : 1, linear: branched) (Scheme 1a).⁶ A similar reaction was described by Willis *et al.* in 2022.⁷

The reaction of aryl sulfide with 1.2 equiv. of alkynol in the presence of a catalytic amount of Rh(nbd)₂BF₄ (5 mol%) produced the corresponding enones **2a/2b** (10 : 2) (Scheme 1b). Ramasastry *et al.* found that PCy₃-catalyzed intramolecular hydroacylation of activated alkynes at room temperature afforded an unexpected product **3** in 78% yield (Scheme 1c).⁸ Inspired by these precedents, we envisioned that *S*-propargylquinoline-3-carbaldehydes may be effective substrates. The catalytic system CuSO₄·5H₂O (10 mol%)/ascorbic acid (15 mol%) furnished the desired 3,9-dimethyl-4*H*-thiopyrano[2,3-*b*]quinolin-4-ones **4** in good yields with a high degree of chemoselectivity (Scheme 1d).

Another atom-economy method for C–C bond formation is metal dimerization of terminal alkynes that can generate high-value 1,3-enynes building blocks.⁹ These structural motifs are found in synthetic conjugated polymers, natural products, and pharmaceuticals with important biological activities.^{10,11} Alkyne dimerization is generally defined as reactions in which a C(sp)–H bond in a terminal alkyne is added to the C≡C bond in another alkyne.¹² Alkyne dimerization can produce a mixture of regio- and/or stereoisomers of 5–7 and/or cyclodimerization or oligomerization side reactions can occur along with it (Fig. 1). Hence, control of the regio- and stereochemistry is essential in this strategy.¹³

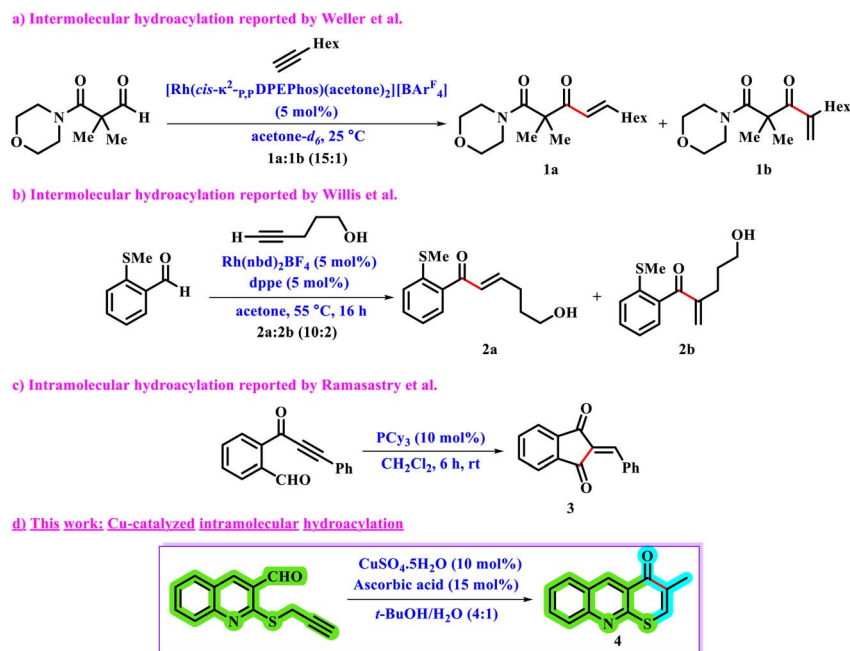
A literature survey shows that several reports have described the use of Fe, Cu, Al, Ru, Co, Rh, Ir, Pd, Y, or Au catalysts to dimerize alkynes. Different reasonable reaction mechanisms are acceptable depending on the type of employed catalyst. Hydro- or carbometallation of monomeric metal acetylide acetylene complexes leads to forming (*E*)-**5** due to both key steps occurring as *syn*-addition. Bimetallic alkyne intermediates generate (*Z*)-**6** because these can undergo anti-additions.

^aFaculty of Chemistry and Petroleum Science, Bu-Ali Sina University, Hamedan, 6517838695, Iran. E-mail: z.tanbakouchian@gmail.com; zolfigi@basu.ac.ir; mzolfigol@yahoo.com

^bDepartment of Chemistry, Faculty of Physics and Chemistry, Alzahra University, Tehran, Iran

^cDepartment of Biomedical and Polymer Chemistry, Faculty of Chemistry, Nicolaus Copernicus University in Torun, Torun, 87-100, Poland

^dDepartment of Chemistry, Faculty of Science, Imam Khomeini International University, Qazvin, 34148-96818, Iran

Scheme 1 Background and significance of current work.

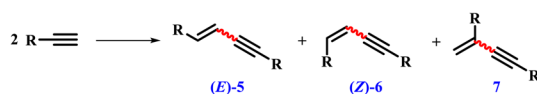


Fig. 1 Possible regio- and/or stereoisomers for alkyne dimerization.

Likewise, regioisomer 7 is formed by head-to-tail dimerization of alkynes through monometallic *syn*-carbometallation and bimetallic hydrometallation as key steps.¹⁴ In this context, Dash and Eisen¹⁵ reported the methylalumoxane (MAO)-catalyzed regio- and chemoselective dimerization of aryl and alkyl-

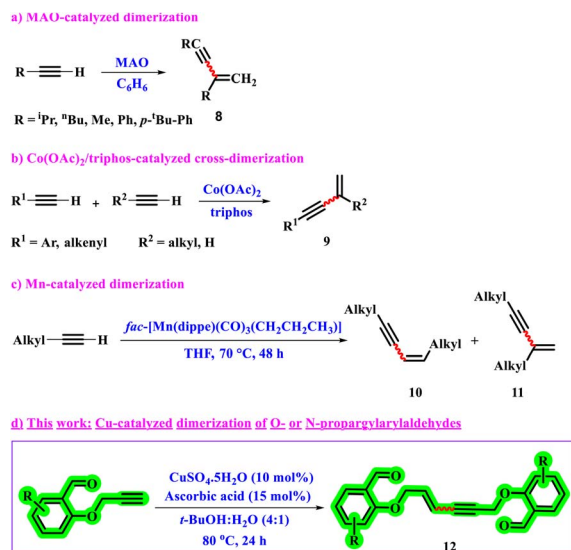
substituted terminal alkynes, leading to the corresponding *gem*-dimers **8** (Scheme 2a). Chen and Li have synthesized a variety of valuable *gem*-1,3-enynes **9** following a Co(II)-catalyzed highly selective cross-dimerization of aryl/alkenyl alkynes and aliphatic alkynes under mild reaction conditions (Scheme 2b).¹⁶ Recently, Kirshner's group¹⁷ has described the use of *fac*-[Mn(dippe)(CO)₃(CH₂CH₂CH₃)] as a precatalyst in the dimerization of terminal aromatic and aliphatic alkynes, affording head-to-head *Z*-1,3-enynes **10** and head-to-tail *gem*-1,3-enynes **11** in high yields with excellent selectivity (Scheme 2c).

Herein, we wish to report a regio- and stereochemical dimerization of *O*- or *N*-propargyl aryl aldehydes using the catalytic system CuSO₄·5H₂O and ascorbic acid. The reactions show excellent regio- and stereoselectivity as mainly the (*E*)-isomer **12** is formed (Scheme 2d).

Results and discussion

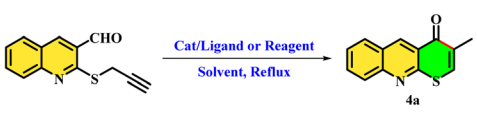
Intramolecular hydroacylation of *S*-propargyl quinoline-3-carbaldehydes to the corresponding α,β-enones

We began our studies by finding the optimal reaction conditions using 2-(prop-2-yn-1-ylthio)quinoline-3-carbaldehyde as the model substrate. The results are listed in Table 1, (SI file). In parallel experiments, the effect of various solvents on the formation of product in the presence of CuSO₄·5H₂O as a catalyst with ascorbic acid as an additive was initially screened (entries 1–12). Among various solvents screened, *t*-BuOH/H₂O (4 : 1) afforded the coupling product with the highest yield in a shorter reaction time (entry 2). The reaction without ascorbic acid was also tested (entry 13). Ascorbic acid is highly effective, and no reaction occurs in its absence. Indeed, ascorbic acid is necessary to reduce Cu(II) to Cu(I).¹⁸ Thus, the reaction was repeated in the presence of CuI as the catalyst (entries 14 and



Scheme 2 Background and significance of this work.

Table 1 Optimization of reaction conditions

					
Entry	Catalyst	Additive	Solvent	Time (h)	Yield (%)
1	CuSO ₄ ·5H ₂ O	Ascorbic acid	<i>t</i> -BuOH	24	NR
2	CuSO₄·5H₂O	Ascorbic acid	<i>t</i>-BuOH/H₂O (4 : 1)	8	85
3	CuSO ₄ ·5H ₂ O	Ascorbic acid	<i>t</i> -BuOH/H ₂ O (1 : 1)	8	54
4	CuSO ₄ ·5H ₂ O	Ascorbic acid	H ₂ O	24	10
5	CuSO ₄ ·5H ₂ O	Ascorbic acid	EtOH	24	NR
6	CuSO ₄ ·5H ₂ O	Ascorbic acid	CH ₃ CN	24	NR
7	CuSO ₄ ·5H ₂ O	Ascorbic acid	CH ₂ Cl ₂	24	NR
8	CuSO ₄ ·5H ₂ O	Ascorbic acid	THF	24	NR
9	CuSO ₄ ·5H ₂ O	Ascorbic acid	Dioxane	24	NR
10	CuSO ₄ ·5H ₂ O	Ascorbic acid	Toluene	24	NR
11	CuSO ₄ ·5H ₂ O	Ascorbic acid	DMF	24	NR
12	CuSO ₄ ·5H ₂ O	Ascorbic acid	DMSO	24	NR
13	CuSO ₄ ·5H ₂ O	—	<i>t</i> -BuOH/H ₂ O (4 : 1)	24	NR
14	CuI	—	<i>t</i> -BuOH/H ₂ O (4 : 1)	24	NR
15	CuI	L-Proline	<i>t</i> -BuOH/H ₂ O (4 : 1)	24	NR

15). Surprisingly, CuI was utterly ineffective and no reaction occurred at all. This matter indicates that the *in situ* generated Cu(I) species from Cu(II) in the presence of ascorbic acid are more active and effective than Cu(I) salt.

The scalability of this reaction was investigated by varying the aryl group in *S*-propargyl aldehydes and the results indicated that the expected products were synthesized in good yields with high regioselectivity in the presence of this catalytic system. As demonstrated in Table 2, *S*-propargyl quinoline-3-carbaldehydes bearing electron-withdrawing groups were generally less reactive and given corresponding products in moderate yields (**4i**, **4j**, and **4h**). In contrast, substrates bearing electron-donating groups on the quinoline ring are more

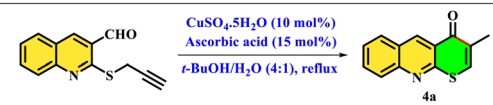
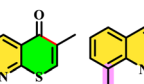
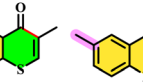
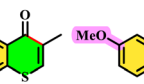
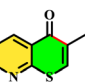
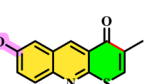
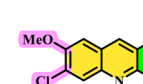
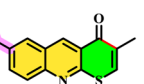
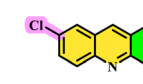
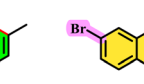
compatible with the reaction, allowing an opportunity for the synthesis of functionalized coupling products in high yields. However, *S*-propargyl aryl aldehydes bearing both electron-donating and electron-withdrawing groups were *endo*-selective regardless of their polarity.

On the basis of the previous reports,¹⁹ the reaction mechanism involves the *in situ* generation of the Cu(I) species by the ascorbic acid, followed by the formation of the metallated intermediate **I** through aldehyde C–H activation and triple bond coordination. Subsequently intermediate **I** deliver product **4** and regenerate Cu(I) in the presence of ascorbic acid for the next catalytic cycle (Fig. 2).

Dimerization of *O*- or *N*-propargylarylaldehydes to the corresponding enynes

In this process, the reaction conditions were firstly optimized by 2-(prop-2-yn-1-yloxy) benzaldehyde as the model substrate in *t*-BuOH : H₂O (4 : 1) under reflux conditions for 24 h. Initially, several Cu(II) salts were examined in the presence of catalytic amounts of ascorbic acid; the results are presented in Table 3. Among all of the tested Cu(II) salts, CuSO₄·5H₂O was the most effective in terms of yield (up to 85%, entry 1). CuI, CuCl₂·2H₂O, and CuBr₂ catalysts were ineffective for dimerizing 2-(prop-2-yn-1-yloxy)benzaldehyde (entries 2–4). Cu(OAc)₂·2H₂O and Cu(NO₃)₂·3H₂O showed very weak catalytic activity, giving trace yields of the desired coupling product (entries 5 and 6). The

Table 2 Substrate's scope of the intramolecular hydroacylation of *S*-propargyl quinoline-3-carbaldehydes

	
 4a , 85%	 4b , 80%
 4c , 87%	 4d , 81%
 4e , 91%	 4f , 69%
 4h , 55%	 4i , 60%
 4j , 52%	

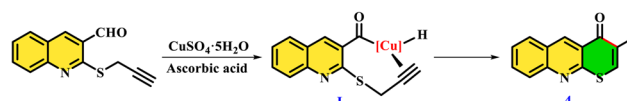


Fig. 2 Proposed mechanistic pathway for intramolecular hydroacylation of *S*-propargyl aryl aldehydes.



Table 3 Optimization of reaction conditions

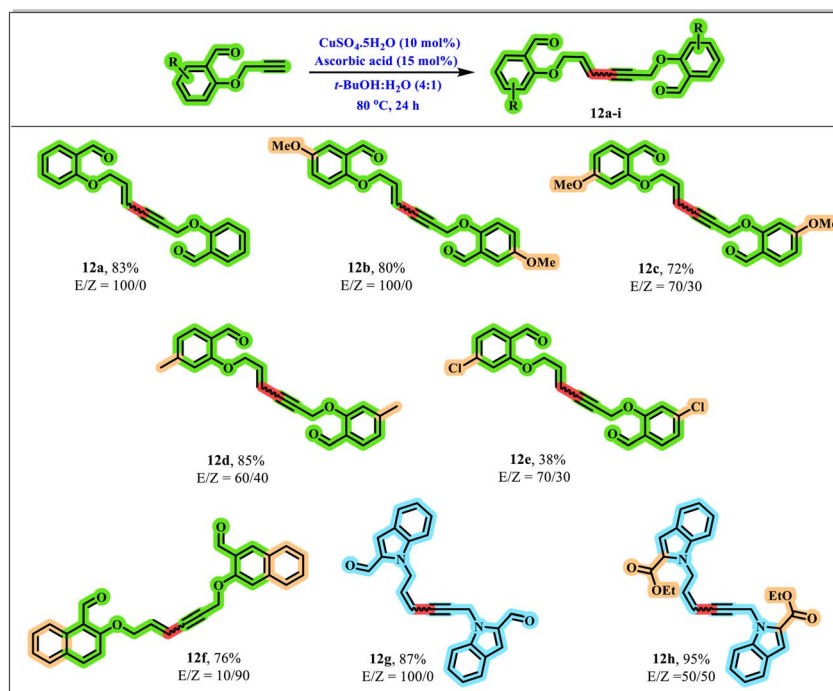
Entry	Catalyst	Additive	Yield (%)
1	CuSO ₄ ·5H ₂ O	Ascorbic acid	85
2	CuI	Ascorbic acid	NR
3	CuCl ₂ ·2H ₂ O	Ascorbic acid	NR
4	CuBr ₂	Ascorbic acid	NR
5	Cu(OAc) ₂ ·2H ₂ O	Ascorbic acid	Trace
6	Cu(NO ₃) ₂ ·3H ₂ O	Ascorbic acid	Trace
7	CuSO ₄ ·5H ₂ O	K ₂ CO ₃ /Ascorbic acid	NR
8	—	K ₂ CO ₃	NR
9	—	<i>t</i> -BuOK	Messy
10	CuI	L-Proline	NR

reaction in the presence of K₂CO₃ was also investigated (entry 7). It was found that the use of a base did not give fruitful results. Also, implementing reactions without a catalyst has no product (entries 8 and 9).

Likewise, the scope of the synthetic procedure was studied using different *O*- or *N*-propargyl arylaldehydes. Table 4 summarizes the dimerization reactions for a series of enynes in moderate to good yields with high regioselectivity. As seen in Table 4, propargyl aryl aldehydes with electron-neutral and electron-rich substituents appear more reactive, providing the corresponding enynes in high yields. Interestingly, the catalytic system shows high regioselectivity control for different substituents regardless of their polarity.

According to the results of experiments and previous reports in the literature,^{14–17} the reaction mechanism of dimerization of a series of *O*- or *N*-propargyl aryl aldehydes was suggested, as displayed in Fig. 3. The reaction is believed to be initiated through the *in situ* formation of Cu(I) ions by reducing Cu(II) ions with ascorbic acid. The catalytic cycle can be started by the interaction of terminal acetylene (**A**) with the *in situ* generated Cu(I) species *via* its triple bond (**B**). Then, the coordination of the acetylide group to the Cu(I) ion by releasing H⁺ would afford the formation of copper(I) acetylide intermediate (**C**). The formation of copper acetylide compounds has also been frequently reported in this type of reactions²⁰ and they have been also structurally identified by X-ray analysis in the literature.²¹ The reaction can precede by coordination of the second terminal acetylene to the copper acetylide intermediate and the C–C bond can be formed by intramolecular rearrangement of the bonds to form (**D**) intermediate. Finally, this intermediate can be protonated to release the corresponding enynes **12**. The Cu(I) species can be regenerated by releasing the enyne product and it can be involved in the next catalytic cycle to form the next molecule of the product.

The structure of one of these enynes (**12h**) was investigated by single crystal X-ray analysis. Structural studies showed that compound **12h** is a (*Z*)-isomer because the two hydrogen atoms of the C18 and C19 carbons are on the same side of the double bond (Fig. 4). The dihedral angle between the planes of the indole rings is 30.55°. The C(O)OEt fragment in both parts of the molecule adopts a similar conformation. The torsion angles C1–C2–O3–C4 and C2–O3–C4–C6 are –153.01(2)° and –176.43(3)°, respectively. While, in the second part of the

Table 4 Substrate's scope of dimerization of *O*- or *N*-propargyl aryl aldehydes

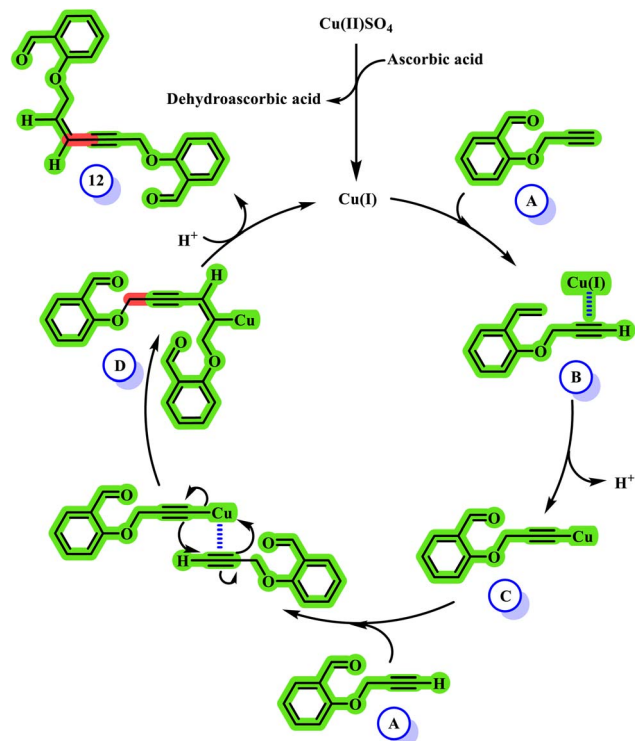


Fig. 3 Proposed mechanistic pathway for dimerization of propargyl aryl aldehydes.

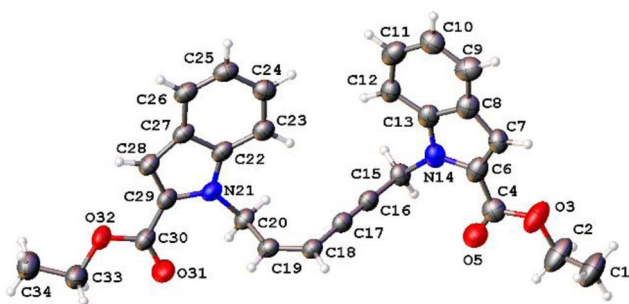


Fig. 4 The asymmetric unit of compound 12h with the thermal ellipsoids at 30% probability level.

molecule, the angles C34–C33–O32–C30 and C33–O32–C30–C29 are equal to $-170.16(2)^\circ$ and $-177.42(2)^\circ$.

The pyrrole ring participates in $\pi \cdots \pi$ interaction with the benzene ring, the $\pi_{N14-C13} \cdots \pi_{C8-C13}$ [$x, -1 + y, z$] distance of $3.7715(2)$ Å. There are also C–H $\cdots\pi$ interactions between the C20–H20B group and pyrrole ring (N21–C29), with a C $\cdots\pi$ distance being $3.3656(12)$ Å. Moreover, analysis of crystal

packing in **12h** revealed the intramolecular C–H \cdots O interactions (Table 5).

Conclusions

In conclusion, the Cu-catalyzed intramolecular hydroacylation of *S*-propargylarylaldehydes in the presence of ascorbic acid gave α , β -enones in high yields and regioselectivity. Meanwhile, homocoupling of *O*- or *N*-propargyl aryl aldehydes renders conjugated enynes in good yields and with high regioselectivity. In both processes, the $\text{CuSO}_4 \cdot 5\text{H}_2\text{O}$ /ascorbic acid catalytic system was the most efficient and effective catalyst for obtaining the corresponding regioisomers. The presented methodologies are highly atom-efficient and regioselective. Propargyl aryl aldehydes bearing electron-donating groups in the aryl moiety are more compatible, generating the corresponding products with high yields. Surprisingly, the catalytic system shows high regioselectivity control for different substituents regardless of their polarity. The main advantages of the catalytic system are the availability and inexpensive copper source, easy separation, high catalytic activity, and selectivity. The required precursors were synthesized according to our very recently reported educational synthetic methodology.²²

Author contributions

Z. Tanbakouchian and M. S. Tonekaboni methodology, validation, investigation. M. A. Zolfigol supervision, resources, project administration, funding acquisition, conceptualization, writing and editing. R. Bikas and A. Kozakiewicz-Piekarz crystallization and single crystal X-ray analysis of the synthesized products, writing and editing.

Conflicts of interest

The authors declare no competing interests.

Data availability

The datasets used and/or analyzed during the current study are available from the corresponding authors on reasonable request.

CCDC 2376902 contains the supplementary crystallographic data for this paper.²³

Supplementary information: experimental section including the details of materials and instruments, synthetic procedures and single crystal X-ray analysis. See DOI: <https://doi.org/10.1039/d5ra07533e>.

Acknowledgements

We are thankful to Bu-Ali Sina University, Nicolaus Copernicus University in Torun and Imam Khomeini International University for the financial support. The author has dedicated this article to three chemistry professors at the University of KwaZulu-Natal, Professor Garrett Krueger, Doctor Glenn E M Maguire and Professor Tawndran, Goandro.

Table 5 Hydrogen bonds in the structure of **12h**

D–H \cdots A	<i>d</i> (D–H)	<i>d</i> (H \cdots A)	<DHA	<i>d</i> (D \cdots A)
C15–H15A \cdots O5	0.99	2.29	121.6	2.932(5)
C20–H20B \cdots O31	0.99	2.33	116.7	2.911(5)



References

- 1 V. Murugesan, A. Muralidharan, G. V. Anantharaj, T. Chinnusamy and R. Rasappan, *Org. Lett.*, 2022, **24**, 8435–8440.
- 2 (a) A. T. Abdulghaffar, H. Zhang, Q. Zhang, Q. Tong, R. Tian, H. Xu, J. Yang and Y. Xu, *Org. Chem. Front.*, 2025, **12**, 346–367; (b) M. Oliva, S. Pillitteri, J. Schörgenhuber, R. Saito, E. V. Van der Eycken and U. K. Sharma, *Chem. Sci.*, 2024, **15**, 17490–17497.
- 3 Z. Zeng, Y. Chen, X. Zhu and L. Yu, *Chin. Chem. Lett.*, 2023, **34**, 107728–107738.
- 4 J. H. Rhlee, S. Maiti, J. W. Lee, H. S. Lee, I. A. Bakhtiyorzoda, S. Lee, J. Park, S. J. Kang, Y. S. Kim, J. K. Seo, K. Myung and S. Y. Hong, *Commun. Chem.*, 2022, **5**, 13.
- 5 T. J. Coxon, M. Fernández, J. Barwick-Silk, A. I. McKay, L. E. Britton, A. S. Weller and M. C. Willis, *J. Am. Chem. Soc.*, 2017, **139**, 10142–10149.
- 6 J. Barwick-Silk, S. Hardy, M. C. Willis and A. S. Weller, *J. Am. Chem. Soc.*, 2018, **140**, 7347–7357.
- 7 N. U. Iwumene, D. F. Moseley, R. D. Pullin and M. C. Willis, *Chem. Sci.*, 2022, **13**, 1504–1511.
- 8 A. Mondal, R. Hazra, J. Grover, M. Raghu and S. S. V. Ramasastry, *ACS Catal.*, 2018, **8**, 2748–2753.
- 9 (a) O. S. Morozov, A. F. Asachenko, D. V. Antonov, V. S. Kochurov, D. Y. Paraschuk and M. S. Nechaev, *Adv. Synth. Catal.*, 2014, **356**, 2671–2678; (b) T. J. Coxon, M. Fernández, J. Barwick-Silk, A. I. McKay, L. E. Britton, A. S. Weller and M. C. Willis, *J. Am. Chem. Soc.*, 2017, **139**, 10142–10149; (c) R. Abonia, D. Insuasty and K. K. Laali, *Molecules*, 2023, **28**, 3379.
- 10 J. Liu, J. Yang, C. Schneider, R. Franke, R. Jackstell and M. Beller, *Angew. Chem., Int. Ed.*, 2020, **59**, 9032–9040.
- 11 S. Ge, V. F. Q. Norambuena and B. Hessen, *Organometallics*, 2007, **26**, 6508–6510.
- 12 C. J. Pell and O. V. Ozerov, *ACS Catal.*, 2014, **4**, 3470–3480.
- 13 P. Zak, M. Bołt, B. Dudziec and M. Kubicki, *Dalton Trans.*, 2019, **48**, 2657–2663.
- 14 C. Pfeffer, N. Wannenmacher, W. Frey and R. Peters, *ACS Catal.*, 2021, **11**, 5496–5505.
- 15 A. K. Dash and M. S. Eisen, *Org. Lett.*, 2000, **2**, 737–740.
- 16 J. F. Chen and C. Li, *ACS Catal.*, 2020, **10**, 3881–3889.
- 17 S. Weber, L. F. Veiros and K. Kirchner, *ACS Catal.*, 2021, **11**, 6474–6483.
- 18 X. Ke, B. Xie, J. Zhang, J. Wang, W. Li, L. Ban, Q. Hu, H. He, L. Wang and Z. Wang, *Nanoscale Adv.*, 2024, **6**, 1135–1144.
- 19 (a) M. K. Majhail, P. M. Ylioja and M. C. Willis, *Chem.–Eur. J.*, 2016, **22**, 7879–7884; (b) T. J. Coxon, M. Fernández, J. Barwick-Silk, A. I. McKay, L. E. Britton, A. S. Weller and M. Willis, *J. Am. Chem. Soc.*, 2017, **139**, 10142–10149.
- 20 N. Heydari, R. Bikas, M. Siczek and T. Lis, *Dalton Trans.*, 2023, **52**, 421–433.
- 21 (a) L.-M. Zhang, G. Zhou, G. Zhou, H. K. Lee, N. Zhao, O. V. Prezhdo and T. C. W. Mak, *Chem. Sci.*, 2019, **10**, 10122–10128; (b) A. Bakhoda, O. E. Okoromoba, C. Greene, M. R. Boroujeni, J. A. Bertke and T. H. J. Warren, *J. Am. Chem. Soc.*, 2020, **142**, 18483–18490; (c) S. Zhang and L. Zhao, *Nat. Commun.*, 2019, **10**, 4848–4858.
- 22 M. A. Zolfigol, S. Azizian, M. Torabi, M. Yarie and B. Notash, *J. Chem. Educ.*, 2024, **101**, 877–881.
- 23 CCDC 2376902: Experimental Crystal Structure Determination, 2025, DOI: [10.5517/ccdc.csd.cc2ksc80](https://doi.org/10.5517/ccdc.csd.cc2ksc80).

